Comparative transcriptome reveals unique pine wood decay strategies in the Sparassis latifolia

Chi Yang
Fujian Academy of Agricultural Sciences
Lu Ma
Fujian Academy of Agricultural Sciences
Donglai Xiao
Fujian Academy of Agricultural Sciences
Xiaoyu Liu
Fujian Academy of Agricultural Sciences
Xiaoling Jiang
Fujian Academy of Agricultural Sciences
Yanquan Lin (lyq-406@163.com)
Fujian Academy of Agricultural Sciences

Article

Keywords: Sparassis latifolia, transcriptome sequencing, pine wood decay, Lipases

Posted Date: July 6th, 2022

DOI: https://doi.org/10.21203/rs.3.rs-1787420/v1

Abstract

Sparassis latifolia is a valuable edible mushroom, growing on fresh pine wood sawdust substrate. However, the mechanistic bases are poorly understood. The gene expression profiles of *S. latifolia* were analyzed from submerged cultures with fresh pine wood sawdust substrate for different times (0 h, 1 h, 6 h, 1 d, 5 d, and 10 d, respectively). The total number of differentially expressed genes (DEGs) identified under pine sawdust inducing was 2,669. And 806, 628, 113, 114, and 94 DEGs were identified at the five time points, respectively. There were 34 genes in common at all inoculated time points, including FAD/NAD(P)-binding domain-containing protein, GMC oxidoreductase, Flavin-containing monooxygenase, and Taurine catabolism dioxygenase. Weighted gene co-expression analysis (WGCNA) were then used to compare the molecular characteristics among the groups and identified that the green module had the highest correlation with group T-6h. There were 48 DEGs out of 58 genes in the green model, including short-chain dehydrogenase, glycoside hydrolase family proteins, Lipase, dienelactone hydrolase, and alpha-L-arabinofuranosidase. Interestingly, lipases are an important group of biotechnological catalysts which catalyze the hydrolysis of Rosin, which is abundant raw material from pine trees. This maybe provides clues into mechanisms that *S. latifolia* can grow on fresh pine wood sawdust substrate.

1. Background

Biodegradation of woody biomass is largely dependent on basidiomycetous fungi (1, 2). In general, wood-decaying fungi can be divided into two categories: (i) white rot, in which the components of plant cells walls are destroyed, and (ii) brown rot, in which lignin is modified by fungi (3, 4). One major degraders of forest biomass is brown rot fungi (2). Wood is degraded by brown-rot fungi using both enzymatic and non-enzymatic processes (5).

It is generally believed that wood-decaying fungi have substrate specificity that defines their ecological niche (6). The mechanisms by which fungi grow on a specific substrate are crucial to understanding both the ecology of fungi and the industrial applications of different feedstocks. Pine trees are a common coniferous group of trees that have a significant ecological and economic significance throughout the world. Sawdust from pine trees, however, is not commonly used since most fungi cannot thrive directly on coniferous wood because of the rosin present in pine trees (7).

Sparassis latifolia is a brown-rot fungus that grows primarily on the stumps or roots of coniferous trees (8, 9), which is the commonly cultivated *Sparassis* species in China (10). A previous study (11) investigated the potential of producing liquid spawn of S. latifolia by submerged fermentation under controlled conditions. It evaluated its ability to colonize on pine sawdust substrate. It was discovered that the transcript levels of genes encoding glycoside hydrolases were mainly governed by carbon source type, while genes involved in hemicellulose degradation were mostly up-regulated (12). However, the mechanism of pine wood decay by *S. latifolia* is still unclear.

In this study, we examined the gene expression of S. latifolia during pine wood decay processing. The sterilized pine sawdust was added into fresh broth cultured mycelia and cultured for 0 h, 1 h, 6 h, 1 d, 5 d, 10 d, respectively. We found that many of the genes involved in known or predicted functions in wood decay were differentiated expressed, with 34 genes (including 17 upregulated and 17 down-regulated genes) in common at all inoculated time points.

2. Results

2.1 RNA sequencing and mapping

To investigate the profile of gene expression during pine sawdust inducing (PSI), samples with three biological replicates were submitted for RNA-Seq. We totally obtained 71.91Gb Clean Data after RNA sequencing for 18 samples with at least 3.38 Gb clean data for each sample. And in each sample, more than 93.84% of bases score Q30 and above (Table 1). The mapping ratio varying from 94.38–95.03% (Table 2).

Table 1
Sequencing data Statistics

Samples	Clean reads	Clean bases	GC Content	%≥Q30
CK-1	15,300,218	4,575,935,026	56.47%	95.23%
CK-2	11,582,063	3,464,275,068	56.38%	95.29%
CK-3	12,389,483	3,705,763,772	56.33%	95.24%
T-10d-1	12,786,507	3,815,880,670	56.59%	94.07%
T-10d-2	13,372,452	3,993,664,028	56.52%	93.96%
T-10d-3	13,205,631	3,943,933,782	56.55%	94.04%
T-1d-1	12,475,495	3,730,823,260	56.41%	94.19%
T-1d-2	12,285,065	3,666,475,380	56.44%	93.84%
T-1d-3	13,389,505	4,004,268,706	56.53%	94.83%
T-1h-1	14,400,608	4,302,919,064	56.30%	94.55%
T-1h-2	15,632,077	4,669,081,164	56.45%	94.30%
T-1h-3	15,326,678	4,578,054,414	56.56%	94.28%
T-5d-1	14,517,067	4,339,936,502	56.51%	95.12%
T-5d-2	11,292,773	3,375,518,776	56.53%	95.09%
T-5d-3	13,043,860	3,895,294,712	56.42%	94.40%
T-6h-1	11,619,691	3,476,037,790	56.54%	95.09%
T-6h-2	13,200,926	3,947,577,998	56.44%	95.32%
T-6h-3	14,818,151	4,427,615,962	56.52%	95.17%

Table 2
Alignment results of each sample

ID	Total Reads	Mapped Reads	Uniq Mapped Reads	Multiple Map Reads	Reads Map to '+'	Reads Map to '-'
CK-1	30,600,436	29,044,147 (94.91%)	27,956,114 (91.36%)	1,088,033 (3.56%)	14,309,892 (46.76%)	14,390,683 (47.03%)
CK-2	23,164,126	21,999,812 (94.97%)	21,170,957 (91.40%)	828,855 (3.58%)	10,831,411 (46.76%)	10,893,389 (47.03%)
CK-3	24,778,966	23,512,915 (94.89%)	22,564,089 (91.06%)	948,826 (3.83%)	11,552,879 (46.62%)	11,635,737 (46.96%)
T-10d-1	25,573,014	24,203,888 (94.65%)	23,253,077 (90.93%)	950,811 (3.72%)	11,908,815 (46.57%)	11,994,367 (46.90%)
T-10d-2	26,744,904	25,242,211 (94.38%)	23,871,260 (89.26%)	1,370,951 (5.13%)	12,287,318 (45.94%)	12,474,309 (46.64%)
T-10d-3	26,411,262	24,982,441 (94.59%)	23,997,669 (90.86%)	984,772 (3.73%)	12,291,848 (46.54%)	12,380,030 (46.87%)
T-1d-1	24,950,990	23,583,112 (94.52%)	22,689,140 (90.93%)	893,972 (3.58%)	11,611,831 (46.54%)	11,681,768 (46.82%)
T-1d-2	24,570,130	23,212,566 (94.47%)	22,354,731 (90.98%)	857,835 (3.49%)	11,429,652 (46.52%)	11,502,280 (46.81%)
T-1d-3	26,779,010	25,375,908 (94.76%)	24,394,245 (91.09%)	981,663 (3.67%)	12,491,402 (46.65%)	12,574,385 (46.96%)
T-1h-1	28,801,216	27,239,764 (94.58%)	25,754,943 (89.42%)	1,484,821 (5.16%)	13,238,036 (45.96%)	13,428,258 (46.62%)
T-1h-2	31,264,154	29,588,505 (94.64%)	28,423,188 (90.91%)	1,165,317 (3.73%)	14,541,255 (46.51%)	14,632,378 (46.80%)
T-1h-3	30,653,356	28,986,961 (94.56%)	27,913,821 (91.06%)	1,073,140 (3.50%)	14,273,055 (46.56%)	14,350,090 (46.81%)
T-5d-1	29,034,134	27,550,568 (94.89%)	26,475,479 (91.19%)	1,075,089 (3.70%)	13,556,480 (46.69%)	13,649,129 (47.01%)
T-5d-2	22,585,546	21,424,342 (94.86%)	20,566,413 (91.06%)	857,929 (3.80%)	10,536,653 (46.65%)	10,615,840 (47.00%)
T-5d-3	26,087,720	24,674,712 (94.58%)	23,606,986 (90.49%)	1,067,726 (4.09%)	12,106,789 (46.41%)	12,212,529 (46.81%)
T-6h-1	23,239,382	22,061,603 (94.93%)	21,251,399 (91.45%)	810,204 (3.49%)	10,870,912 (46.78%)	10,925,195 (47.01%)

ID	Total Reads	Mapped Reads	Uniq Mapped Reads	Multiple Map Reads	Reads Map to '+'	Reads Map to '-'
T-6h-2	26,401,852	25,089,074 (95.03%)	24,158,588 (91.50%)	930,486 (3.52%)	12,362,925 (46.83%)	12,421,200 (47.05%)
T-6h-3	29,636,302	28,121,984 (94.89%)	27,061,825 (91.31%)	1,060,159 (3.58%)	13,845,390 (46.72%)	13,924,141 (46.98%)

2.2 Differential gene expression and functional enrichment analysis

To further confirm the quality of RNA-seq, PCA and Pearson correlation analysis were performed. Based on the correlation results for samples in Fig. 1A and 1B, CK-1, T-1d-3, and T-5d-2 were excluded for further analysis. During identifying differentially expressed genes (DEGs), Fold Change (FC) ≥ 2 and FDR < 0.01 were used as the screening criteria. In total, 2,659 DEGs were identified under pine sawdust inducing; we identified 1,073, 520, 385, 424, and 257 DEGs at the five time points, respectively (Table 3). There were 34 genes in common at all inoculated time points, including 17 upregulated and 17 down-regulated genes (Fig. 1C and Table S1). Most of these common DEGs were function unknown hypothetical protein.

Table 3
The number of DEGs at the five time points compared to Control group.

Groups	DEGs_total	DEGs_up	DEGs_down
1 h	257	154	103
6 h	424	294	130
1 d	385	176	209
5 d	520	306	214
10 d	1073	481	592

These 34 genes were involved in biological processes (BP) associated metabolic process, cellular process, single-organism process, localization, and biological regulation (Fig. 2A). GO cellular component (CC) analysis showed that the 34 genes were enriched in membrane and membrane part. In addition, the molecular function (MF) of these 34 genes were mainly associated with catalytic activity, binding, transporter activity, and nucleic acid binding transcription factor activity. These genes were enriched in “General function prediction only”, “Coenzyme transport and metabolism”, “Translation, ribosomal structure and biogenesis”, et al COG classifications (Fig. 2B). Meanwhile, eggNOG analysis revealed that “Function unknown” was the most enriched group, followed by “Transcription”, “Energy production and

conversion", and some "transport and catabolism" groups (Fig. 2C). KOG classifications put these genes into 2 functional groups (Fig. 2D). The largest cluster was "General function prediction only", and followed by "Secondary metabolites biosynthesis, transport and catabolism". However, there were no significantly enriched KEGG pathways for these 34 genes.

2.3 Weighted correlation network analysis

Through correlation analysis, the gene modules related to specific sample traits could quickly screened from the data. Specifically, we identified 8 functional modules related to PSI by WGCNA. As a result, clustering analysis was carried out on 634 genes using the average linkage method and Pearson's correlation method. The soft threshold power value of β = 15 was selected to obtain a scale-free co-expression network (Fig. 3A). Seven modules were identified based on average hierarchical clustering and dynamic tree clipping (Fig. 3B and 3C). As shown in Fig. 3D, the green module had the highest correlation with group T-6h (cor = 0.98) and was therefore selected for subsequent analysis. After performing the gene significance against module membership, we observed that genes with high module memberships tended to have high gene significance in the green module (cor = 0.95, $P < 5.5e\text{-}30$; Fig. 3E).

2.4 Function annotation of DEGs in green module

There were 58 genes in the green module. In order to screen out the core genes that are more relevant and highly correlated to the module eigengene, we then checked the gene expression in T-6h group compared to Control group and 48 DEGs were screened out (Table S2). In order to systemically investigate the function and pathway of the green module, we further performed GO and KEGG pathway enrichment analysis. According to the GO annotation, the biological process categories included metabolic process, cellular process, single-organism process, and response to stimulus. In addition, cellular component categories were enriched in cell, cell part, organelle, membrane, membrane part, and organelle part. Similarly, the molecular function categories included catalytic activity, binding, molecular transducer activity, and signal transducer activity (Fig. 4B). It was further noted that the genes in the green module were assigned to MAPK signaling pathway-yeast, biosynthesis of antibiotics, amino sugar and nucleotide sugar metabolism, steroid biosynthesis, terpenoid backbone biosynthesis, and starch and sucrose metabolism (Fig. 4A). The largest cluster enriched in COG, eggNOG, and KOG were "Lipid transport and metabolism", "Function unknown", and "Posttranslational modification, protein turnover, chaperones", respectively (Fig. 4C-4E).

2.5 Expression validation of hub genes

By literature search, 8 genes related to wood decay were selected for further validation. The module membership of selected genes was ranged from 0.7780 to 0.9777 (Fig. 5A). qRT-PCR was used to quantitatively validate the sequencing data. GAPDH was selected as the reference gene because of its stable expression level based on our previous study (27). As shown in Fig. 5B, 7 out 8 genes had the similar expression pattern to the RNA-seq results.

3. Discussion

Mushroom-forming fungi are important wood-degraders in global carbon cycling. However, wood-decaying fungi tend to have characteristic substrate ranges. Most wood-decaying fungi are unable to colonize coniferous wood directly due to the rosin resent in pine trees (7). There were only little studies that focus on the pine wood decay, the fungi included *Fomitopsis pinicola* (6, 28), *Antrodia sinuosa* (28), *Postia placenta* (28), *Wolfiporia cocos* (28), *Laetiporus sulphureus* (28), *Daedalea quercina* (28), *Rhodonia placenta* (29) and *Schizophyllaceae* (30). However, all these studies were not indicated that the pine wood used was fresh.

Sawdust from fresh pine trees is not commonly utilized, due to the rosin resent in pine trees, most fungi cannot colonize coniferous wood directly (7). However, our previous study revealed that *S. latifolia* can grow on fresh pine wood sawdust substrate(11, 12). So, we hypothesized that there were some special genes in *S. latifolia* to ensure it could grow on fresh pine wood. In our results, the 34 common DEGs in all time points were searched out (Fig. 1C, Table S1). Some of these DEGs were reported in previous studies, including GMC oxidoreductase (EVM0000788) (28), FAD/NAD(P)-binding domain-containing protein (EVM0008017) (6), Flavin-containing monooxygenase (EVM0013062) (5), and Taurine catabolism dioxygenase (EVM0008301) (5). However, most DEGs were function unknown or had no related function report.

Based on the results of WGCNA, the green module had the highest correlation with group T-6h (Fig. 3D). 48 out of 58 genes in the green model were significantly differentiated expressed under 6h pine sawdust inducing (Table S2). Among these genes, short-chain dehydrogenase (EVM0011942, EVM0008874) (5), glycoside hydrolase family proteins (EVM0005932, EVM0009669), Lipase (EVM0012460) (5, 6), dienelactone hydrolase (EVM0004895) (5), and alpha-L-arabinofuranosidase (EVM0009669) (5) were wood decay related. But the DEGs here had no common genes with the 34 common DEGs in all treatment groups compared to control.

Rosin is an abundant raw material from pine trees, resulting in most fungi are unable to colonize coniferous wood directly (7). Lipases are an important group of biotechnological catalysts which catalyze the hydrolysis of triglycerides into free fatty acids and glycerol (31). In the results of this study, Lipase gene (EVM0012460) was significantly up regulated (Fig. 3d), which was also up regulated in *Fomitopsis pinicola* (5, 6). This maybe one of the reasons that *S. latifolia* can grow on fresh pine wood sawdust substrate.

4. Materials And Methods

4.1 Strain and sample preparation

The *S. latifolia* strain SP-C was preserved at the Institute of Edible Mushroom, Fujian Academy of Agricultural Sciences (Fuzhou, China). Potato dextrose agar (PDA) slants were used to grow the strain,

and the seed culture medium contained potato (20%), glucose (2%), and fish peptone (0.3%). The mycelia were activated for ten days at 25°C in darkness on a PDA slant. Mycelial plugs (2 mm in diameter) were cultured with 100 mL of liquid media in 250 mL flasks in a rotatory incubator at 25°C with shaking at 150 rpm/min for 9 days in darkness. After homogenizing, the spawn was transferred to a new 250 mL flasks containing 100 mL of liquid media and cultured for 2 d. Then, 1 g sterilized fresh pine sawdust was added at different time, so that the pine sawdust inducing time were 0 h, 1 h, 6 h, 1 d, 5 d, and 10 d, respectively. Finally, the strains were collected at the same time by filtering to remove sawdust.

4.2 RNA sequencing

Total RNA was isolated by using TRIzol (Invitrogen, USA) according to the manufacturer's instructions. Agilent 2100 Bioanalyzeror SMA3000 was used to measure RNA purity, concentration, and RNA integrity number. RNA-Seq was performed as previously described (13). Briefly, From total RNA, mRNA was enriched using poly (T) + oligo beads, eluted with Tris-HCl buffer, then fragmented using RNA fragmentation kits (Ambion, Austin, TX, USA). A random hexamer primer and M-MuLV Reverse Transcriptase were used to make first strand cDNA. Subsequently, second strand cDNA synthesis was carried out using DNA Polymerase I and RNase H. By using exonuclease/polymerase, the remaining overhangs were converted into blunt ends. In order to prepare for hybridization, NEBNext Adaptors with hairpin loop structure were ligated after 3'-adenylation of DNA fragments. A purification procedure was performed using AMPure XP (Beckman Coulter, Beverly, USA) to select cDNA fragments of 240 bp or less in length from the library fragments. With size-selected, adaptor-ligated cDNA, 3 ul USER Enzyme (NEB, USA) was used at 37°C for 15 min and then at 95°C for 5 min prior to PCR. Next, PCR was performed using Phusion DNA polymerase, Universal PCR primers, and Index (X) primer. Final steps included purifying PCR products (AMPure XP system) and assessing the quality of the libraries (Agilent Bioanalyzer 2100 system). In accordance with the manufacturer's instructions, the indexed samples were clustered using TruSeq PE Cluster Kit v4-cBot-HS (Illumia) on a cBot Cluster Generation System. Using an Illumina platform, paired-end reads were generated from the library preparations after cluster generation.

4.3 Read mapping, annotation, and quantification of gene expression

By using Cutadapt, adaptor sequences and low-quality sequence reads were removed from the data sets (14). Clean reads were generated after raw sequences were processed. These clean reads were mapped to the reference genome sequence of *S. latifolia* (15) by Hisat2 tools (version 2.0.4) (16). Reads were aligned to the reference genome and then assembled into transcripts by StringTie (version 1.3.3b) using default parameters (version 2.0.6) (17). Transdecoder (version 2.0.1) were used to predict coding sequences. Gene function was annotated based on seven databases, including Nr (NCBI non-redundant protein sequences), Nt (NCBI non-redundant nucleotide sequences), Pfam (Protein family), KOG/COG (Clusters of Orthologous Groups of proteins), Swiss-Prot (A manually annotated and reviewed protein sequence database), KO (KEGG Ortholog database), and GO (Gene Ontology). Then, picard-tools v1.41 and samtools v0.1.18 were used to sort, remove duplicated reads and merge the bam alignment results of each sample. Gene expression patterns were quantified using STAR-RSEM algorithm (version 4.1). The

mapped read numbers were calculated and normalized by RESM-based algorithm in the Trinity package (18).

4.4 Differential expression analysis

Principal component analysis (PCA) was utilized to reduce and summarize large datasets while illustrating relationships between samples based on co-variance of the data being examined. The mapped reads of the 500 genes that had the largest coefficients of variation based on the fragments per kilobase of transcripts per million (FPKM)(19) were used for principal component analysis (PCA) and heat mapping with unsupervised clustering. Based on read counts, the pair-wise spearman correlation between any pair of samples was calculated. DESeq2 R package was used to analyze the differential expression (20). Genes with |FoldChange|> 2.0 and adjusted P-value < 0.01 were assigned as differentially expressed.

4.5 WGCNA analysis

The weighted gene co-expression network analysis (WGCNA) was used to identify the functional modules, which has advantages to find the complex relationships between relating modules and associated with traits(21). Specifically, the lowest soft-thresholding power for which the scale-free topology fit was selected. The topological overlap matrix (TOM) similarity was calculated using the power and expression data of differentially expressed genes. The clustering tree structure of the TOM were constructed by hierarchical clustering method. Different branches of the clustering tree represent different gene modules, and different colors represented different modules. Genes with similar patterns were grouped into one module according to the weighted correlation coefficients of genes. The correlation between co-expression modules and traits was estimated based on the phenotypic information of pine wood sawdust inducing time of 0 h, 1 h, 6 h, 1 d, 5 d and 10 d. A significant co-expression module highly related to traits was identified. Module–trait relationships were computed by Pearson's correlation tests, and $P < 0.05$ was defined significant correlation. WGCNA analysis was performed using BMKCloud (www.biocloud.net). Gene Ontology (GO) enrichment analysis was implemented by the GOseq R packages based Wallenius non-central hyper-geometric distribution (22). We used KOBAS (23) software to test the statistical enrichment of differential expression genes in KEGG pathways (24). The GO and KEGG were plotted was plotted by ImageGP (http://www.ehbio.com/ImageGP/index.php/Home/Index/index.html), a free online platform for data analysis and visualization(25).

4.6 Gene expression validation by quantitative RT-PCR

Gene expression analysis was performed by qRT-PCR as previously described (26). Briefly, total RNA was isolated using TRIzol reagent (Invitrogen) and then reverse transcribed with PrimeScript™ II 1st Strand cDNA Synthesis Kit (Takara, Japan) following the manufacturer's instructions. cDNA was quantified using SYBR Premix Ex Taq kit (Takara, Japan) on an ABI QuantStudio instrument. The GAPDH gene was selected as control (27). Primers used in this study were described in Supplementary Table S3. The reaction mixture contained 4.5 μL cDNA, 0.5 μL primers (10 μM), 12.5 μL 2×SYBR Premix Ex Taq, and

ddH_2O up to 20 µl. The thermal cycling conditions were: 95°C for 1 min; followed by 40 cycles of 10 s at 95°C, 34 s at 60°C; and 60°C for 1 min, and 60°C to 95°C for the dissociation curve analyses. Three biological replicates were used. qRT-PCR data were presented as mean ± SD. The relative gene expression was calculated using the $2^{-\Delta\Delta CT}$ method. The statistical significance of differences was assessed using one-way ANOVA in Office Excel 2016. The significance was set with *P < 0.05, **P < 0.01.

Declarations

Availability of data and material: The RNA-Seq data had been deposited in NCBI under accession GSE173822. To review GEO accession GSE173822, please go to https://www.ncbi.nlm.nih.gov/geo/query/acc.cgi?acc=GSE173822, and Enter token cpadicqqdbklrsv into the box.

Competing interests: The authors declare that the research was conducted in the absence of any commercial or financial relationships that could be construed as a potential conflict of interest.

Funding: This work was supported by the projects from Fujian Academy of Agricultural Sciences (CXTD2021016-2, XTCXGC2021007), Natural Science Foundation of Fujian province of China (2020J011378), Seed Industry Innovation and Industrialization Project of Fujian Province (zycxny2021011).

Authors' contributions: Conceptualization, C.Y. and Y.Q. L.; Data curation, L. M., D.L. X. and X.Y. L.; Formal analysis, L.M.; Funding acquisition, C.Y., L.M. and D.L. X.; Investigation, C. Y., L. M. and X.L. J.; Methodology, D.L. X.; Project administration, C. Y.; Supervision, Y.Q. L.; Validation, D.L. X., X.Y. L. and X.L. J.; Visualization, D.L. X. and X.Y. L.; Writing – original draft, C. Y.; Writing – review & editing, C. Y., L. M., X.Y. L. and Y.Q. L. All authors have read and agreed to the published version of the manuscript.

Acknowledgements: We are grateful to the members of the lab for their assistance and helpful discussions. We sincerely thank the editor and reviewers for critically evaluating this manuscript and providing constructive comments for its improvement.

References

1. Bagley ST, Richter DL. Biodegradation by Brown Rot Fungi. Industrial Applications. 2002.
2. Goodell B, Nicholas DD, Schultz TP, Meeting ACS. Wood Deterioration and Preservation: Advances in Our Changing World: Wood Deterioration and Preservation: Advances in Our Changing World; 2003.
3. Eriksson KE, Blanchette RA, Ander P. Microbial and Enzymatic Degradation of Wood and Wood Components: Microbial and Enzymatic Degradation of Wood and Wood Components; 1990.
4. Blanchette, Robert A. Degradation of the lignocellulose complex in wood. Canadian Journal of Botany. 1995;73:S999-S1010.

5. Sista Kameshwar AK, Qin W. Systematic metadata analysis of brown rot fungi gene expression data reveals the genes involved in Fenton's reaction and wood decay process. Mycology. 2020;11(1):22-37.
6. Wu B, Gaskell J, Held BW, Toapanta C, Vuong T, Ahrendt S, et al. Substrate-Specific Differential Gene Expression and RNA Editing in the Brown Rot Fungus Fomitopsis pinicola. APPL ENVIRON MICROB/3823. 2018;84(16):e00991-18.
7. Croan SC. Conversion of conifer wastes into edible and medicinal mushrooms. FOREST PROD J/0481. 2004;54(2):68-76.
8. Kim SR, Kang HW, Ro HS. Generation and Evaluation of High beta-Glucan Producing Mutant Strains of Sparassis crispa. MYCOBIOLOGY/0573. 2013;41(3):159-63.
9. Dong JL, Min CJ, Jo AR, Choi HJ, Kim KS, Chi YT. Noble strain of Sparassis latifolia produces high content of β-glucan. Asian Pacific Journal of Tropical Biomedicine. 2015.
10. Yang C, Ma L, Ying ZH, Jiang XL, Lin YQ. Sequence Analysis and Expression of a Blue-light Photoreceptor Gene, Slwc-1 from the Cauliflower Mushroom Sparassis latifolia. CURR MICROBIOL/1519. 2017;74(4):469-75.
11. Ma L, Lin YQ, Yang C, Ying ZH, Jiang XL. Production of liquid spawn of an edible mushroom, Sparassis latifolia by submerged fermentation and mycelial growth on pine wood sawdust. SCI HORTIC-AMSTERDAM/1538. 2016;209(19):22-30.
12. Xiao DL, Ma L, Yang C, Lin YQ. Transcriptome analysis of Sparassis latifolia cultivated with different carbon sources. Microbiology China. 2019;046(007):1654-61.
13. Tong X, Zhang H, Wang F, Xue Z, Cao J, Peng C, et al. Comparative transcriptome analysis revealed genes involved in the fruiting body development of Ophiocordyceps sinensis. PEERJ/2183. 2020;8:e8379.
14. Martin M. Cutadapt removes adapter sequences from high-throughput sequencing reads. Embnet Journal. 2011;17(1).
15. Yang C, Ma L, Xiao DL, Liu XY, Jiang XL, Ying ZH, et al. Chromosome-scale assembly of the Sparassis latifolia genome obtained using long-read and Hi-C sequencing. G3 Genes|Genomes|Genetics. 2021;11(8):jkab173.
16. Kim D, Langmead B, Salzberg SL. HISAT: a fast spliced aligner with low memory requirements. NAT METHODS/25328. 2015;12(4):357-60.
17. Pertea M, Pertea GM, Antonescu CM, Chang TC, Mendell JT, Salzberg SL. StringTie enables improved reconstruction of a transcriptome from RNA-seq reads. NAT BIOTECHNOL/43113. 2015;33(3):290-5.
18. Pertea M, Kim D, Pertea GM, Leek JT, Salzberg SL. Transcript-level expression analysis of RNA-seq experiments with HISAT, StringTie and Ballgown. NAT PROTOC/9646. 2016;11(9):1650-67.
19. Anders S, Huber W. Differential expression analysis for sequence count data. GENOME BIOL/11313. 2010;11(10):R106.

20. Love MI, Huber W, Anders S. Moderated estimation of fold change and dispersion for RNA-seq data with DESeq2. GENOME BIOL/11313. 2014;15(12):550.
21. Zhang X, Cui Y, Ding X, Liu S, Han B, Duan X, et al. Analysis of mRNA-lncRNA and mRNA-lncRNA-pathway co-expression networks based on WGCNA in developing pediatric sepsis. BIOENGINEERED/187. 2021;12(1):1457-70.
22. Young MD, Wakefield MJ, Smyth GK, Oshlack A. Gene ontology analysis for RNA-seq: accounting for selection bias. GENOME BIOL/11313. 2010;11(2):R14.
23. Mao X, Cai T, Olyarchuk JG, Wei L. Automated genome annotation and pathway identification using the KEGG Orthology (KO) as a controlled vocabulary. BIOINFORMATICS/5766. 2005;21(19):3787-93.
24. Kanehisa M, Araki M, Goto S, Hattori M, Hirakawa M, Itoh M, et al. KEGG for linking genomes to life and the environment. NUCLEIC ACIDS RES/9202. 2008;36(Database issue):D480-4.
25. Chen T, Liu Y-X, Huang L. ImageGP: An easy-to-use data visualization web server for scientific researchers. iMeta. 2022;1(1):e5.
26. Yang C, Ma L, Ying ZH, Jiang XL, Lin YQ. Sequence Analysis and Expression of a Blue-light Photoreceptor Gene, *Slwc-1* from the Cauliflower Mushroom Sparassis latifolia. CURR MICROBIOL/1519. 2017;74(4):469-75.
27. Yang C, Ma L, Xiao DL, Ying ZH, Jiang XL, Lin YQ. Identification and Evaluation of Reference Genes for qRT-PCR Normalization in *Sparassis latifolia* (Agaricomycetes). INT J MED MUSHROOMS/1357. 2019:DOI: 10.1615/IntJMedMushrooms.2019030106.
28. Wu B, Gaskell J, Zhang J, Toapanta C, Ahrendt S, Grigoriev IV, et al. Evolution of substrate-specific gene expression and RNA editing in brown rot wood-decaying fungi. The ISME journal. 2019;13(6):1391-403.
29. Belt T, Altgen M, Makela M, Hanninen T, Rautkari L. Cellular level chemical changes in Scots pine heartwood during incipient brown rot decay. Sci Rep. 2019;9(1):5188.
30. Almási É, Sahu N, Krizsán K, Bálint B, Kovács GM, Kiss B, et al. Comparative genomics reveals unique wood-decay strategies and fruiting body development in the Schizophyllaceae. The New phytologist. 2019;224(2):902-15.
31. Rajan A, Abraham TE. Enzymatic modification of cassava starch by bacterial lipase. Bioprocess Biosyst Eng. 2006;29(1):65-71.

Figures

Figure 1

The differentially expressed genes (DEGs) in PSI. (A) PCA plot. (B) Correlation heat map. (C) The Venn diagram for the DEGs shared between the five time points.

Figure 2

function annotation of the 34 common DEGs. (A) GO classification. (B) COG functional categories. (C) eggNOG functional categories. (D) KOG functional categories

Figure 3

Construction of WGCNA analysis. (A) The soft-threshold power versus scale-free topology model fit index and mean connectivity. The left image shows the scale-free fit index (*y*-axis) as a function of the soft-thresholding power (*x*-axis). The right image shows the average connectivity (degree, *y*-axis) as a function of the soft-thresholding power (*x*-axis). (B) Heat map of the correlation between modules and traits. (C) Module clustering tree. (D) Heatmap shows correlations of module-related genes and the treatment time of pine sawdust. (E) A scatter plot of gene significance (GS) vs. module membership (MM) in the green module.

Figure 4

Function annotation of DEGs in green module. (A) KEGG pathway enrichment analysis in the green module. The vertical axis represents the enriched pathways, and the horizontal axis represents the ratio of enriched genes in the module. The point size represents the gene number enriched in the pathway and the color represents the q-Value. (B) GO functional enrichment analysis. (C) COG functional categories. (D) eggNOG functional categories. (E) KOG functional categories

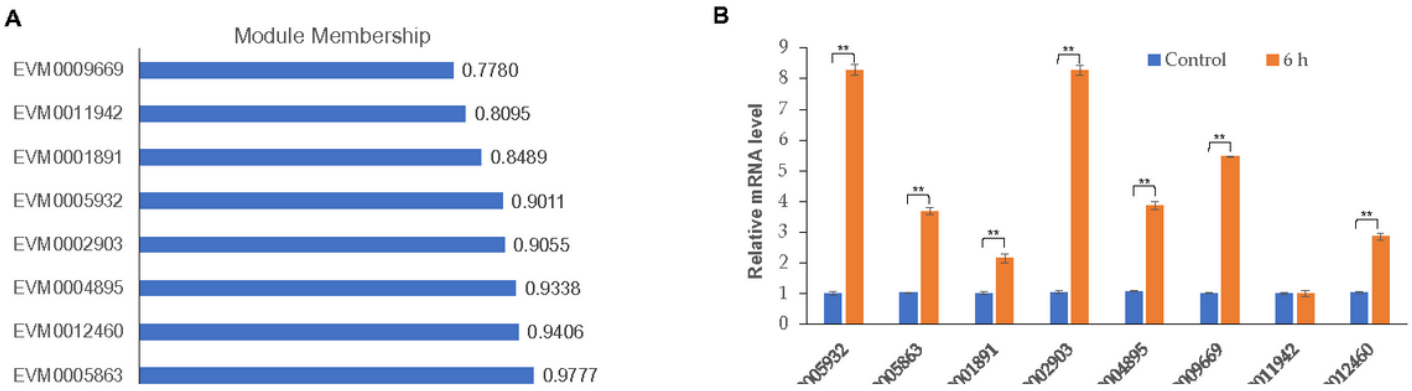

Figure 5

Expression validation of hub genes. (A) Module membership of selected genes. (B) Expression validation of selected genes by qRT-PCR.

Supplementary Files

This is a list of supplementary files associated with this preprint. Click to download.

- TableS.xlsx